Minimum and Complete Fluidization Velocity for Sand-Palm Shell Mixtures, Part I: Fluidization Behaviour and Characteristic Velocities

V.S. Chok
Department of Chemical Engineering,
Universiti Teknologi PETRONAS,
31750 Tronoh, Perak, Malaysia
chokvuisoon@yahoo.com.sg

A. Gorin, H.B. Chua
School of Engineering and Science,
Curtin University of Technology Sarawak Campus,
CDT 250, 98009 Miri, Sarawak, Malaysia
alexander.g@curtin.edu.my

Abstract— **Palm shell on its original state cannot be fluidized solely. However, mixing palm shell with a second fluidizable material can facilitate proper fluidization. The minimum and complete fluidization velocity (U_{mf} and U_{cf}) for sand/palm shell binary mixtures have been studied in a novel design of partitioned reactor known as compartmented fluidized bed gasifier (CFBG). The pilot scale reactor ID is 66cm with 60:40 cross sectional area ratio for combustor and gasifier respectively. Each compartment consists of a pair of devices at the partitioning wall for internal solid circulation. The bed materials constitute of sand and palm shell up to 15 weight percent (wt.%). The particle size and density ratio for palm shell and sand are about 5÷53 and 0.55 respectively. Despite of the unique reactor feature, the mixture bed pressure drop profiles are closely resemble to those observed in the laboratory scale cylindrical column. These profiles have indicated that proper fluidizations are attainable for the binary mixtures in both compartments but vary with the sand size, palm shell size and weight percent in the mixtures. It was found that partial fluidization occurred for the smallest sand size with any palm shell size and weight percent in the gasifier. Poor fluidization was also found with the same sand in the combustor but limited to the largest palm shell and higher weight percent. The U_{mf} and U_{cf} values increase with the increase of palm shell size and weight percent in both compartments and are in tandem with the increase of effective particle diameter. However, although increase in the sand size also increases the effective particle diameter, the characteristic velocities show both increasing and decreasing trends. It is deduced that the mechanism in attaining/maintaining binary mixture fluidization in the gasifier is primarily contributed by the gas-to-particle interaction since particle-particle interaction is suppressed due to segregation. To the contrary, the fluidization mechanism in the combustor depends largely on the particle-particle interaction and this also promoted by better mixing condition. The results on the ratio and difference on the characteristic velocities (U_{cf} /U_{mf} and U_{cf}–U_{mf}) of the binary mixtures as well as the ratio of binary mixture to pure sand characteristic velocities (U_{mf}/U_{mf}^{o} and U_{cf}/U_{cf}^{o}) support these findings.**

Keywords-component; binary mixtures, biomass fluidization, compartmented fluidized bed; minimum fluidization velocity; complete fluidization velocity

I. INTRODUCTION

The feasibility studies of palm oil waste including palm shell as biomass gasification feedstock have been well reported in [1]-[2]. The laboratory analyses on the physical and chemical characteristics have also been well documented in [3]-[4] citing palm oil solid residual as an ideal choice for thermo-chemical conversion. Hence, the main obstacles that need to be resolved now are on the technical and technological challenges as well as on its implementation as the gasification feedstock.

A preceding work on the CFBG fluidization behaviour and its characteristic velocities using only common bed material i.e. sand of various sizes and distribution was examined in [5]. In that work, it is confirmed that the hydrodynamic characteristic of CFBG is closely resemble to those reported in cylindrical fluidized bed of laboratory scale despite of its distinctive geometrical features. It then permits the used of the bed pressure profile to determine the characteristic velocities i.e. the minimum and complete fluidization velocity (U_{mf} and U_{cf}). The present work is a successive study that involves the addition of a locally available biomass residual, i.e. palm shell, into these sands to form a binary component system with large difference in size and density. Palm shell cannot be fluidized solely. Palm shell is considered as Geldart D particle, a classification for spouting bed material. However, mixing palm shell with a second fluidizable material (sand) can facilitate proper fluidization. Based on the criteria in [6], palm shell can be considered as a flotsam (tends to float) while sand is a jetsam (tends to sink), although it actually varies depending on the particle size and density, even their relative proportions. Some interesting works in [7]-[8] on hydrodynamic studies of sand-palm shell mixtures are available. They are, however confined to single palm shell and/or sand size.

The present paper reports the minimum and complete fluidization velocity for sand-palm shell mixtures and detailed the effects of sand sizes, palm shell sizes and weight percent. It also discussed the insights derived from the various relationships of the characteristic velocities to support the understanding of mixture fluidization mechanism in different compartments.

Authors would like to thank the Ministry of Science, Technology and Innovation and Malaysia Palm Oil Board for the financial support.

II. EXPERIMENTAL

A. Apparatus

As the apparatus for this study is the same as described in [1], only a brief description is included here. A schematic of the experimental setup is illustrated in Fig. 1. The cold flow model as shown in Fig. 2 has a 0.66 ID and is divided into 2 compartments i.e. combustor and gasifier by a vertical wall in 2:1 cross-sectional area ratio [9]. Two pairs of devices known as v-valve and riser are available for internal solid circulation between the respective beds. In the present studies, only the beds were subjected to air for fluidization. The flow rates were regulated using rotameters (measure up to 2600 liter per minute) to maintain the bubbling mode of fluidization. Pressure drops were measured using water manometers at 3 different locations for total pressure drop (ΔP_t), across distributor (ΔP_d) and bed (ΔP_b) respectively.

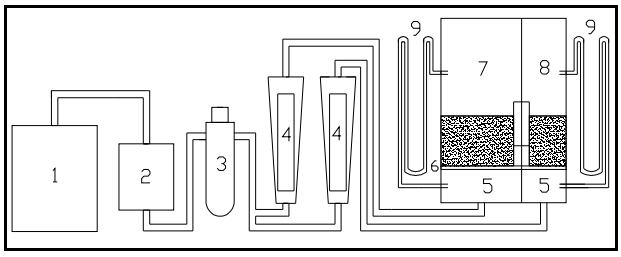

Figure 1. Experimental setup - 1: compressor; 2: dryer; 3: pressure regulator; 4: rotameter; 5: plenum; 6: perforated distributor; 7: combustor; 8: gasifier; 9: manometer [9]

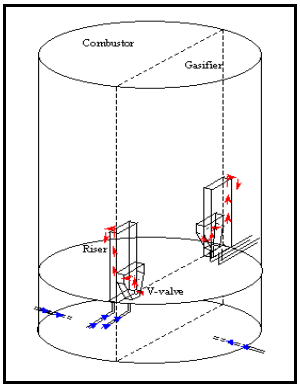

Figure 2. Isometric view of CFBG [9]

The effective diameters, D_e are computed as 25.7 and 41.3 cm for gasifier and combustor respectively [9]. The presence of v-valve and riser in both compartments has been addressed when considering the effective bed diameter.

B. Material

In considering the typical bed aspect ratio of 1-2, the experiments were carried out in both of the compartments at 0.4 m static bed height[1]. Large amount of bed material is used, i.e. at 77 and 101 kg respectively. Large amount of the biomass is also needed, up to 15 kg of each sieved size.

The weight percent of various palm shell sizes is shown in Fig. 3. The biomass residuals were obtained from a palm oil mill and underwent natural drying prior utilization. The final moisture content was found to be 8-10 wt%. It can be clearly seen that the biomass consists mostly larger particles of 3.56 and 7.13 mm. 4 different sizes of palm shell are used in this study, excluding the smallest palm shell that mostly consists of loose fiber as shown in Table 1. 4 different types of sand sizes are selected as the inert materials. The physical properties of the sand and palm shell are given in Table 1.

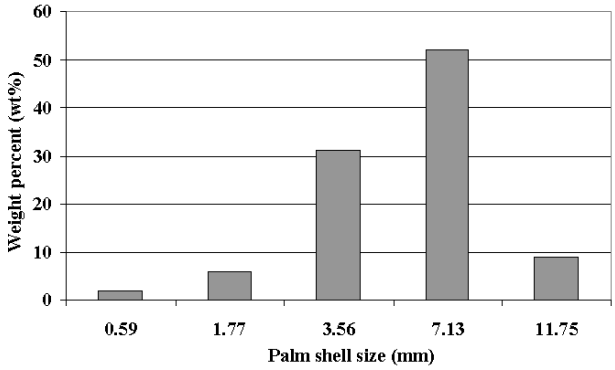

Figure 3. Weight percent of various palm shell size from mill

TABLE I. PALM SHELL AND SAND PROPERTIES

Properties	Palm shell	Sand
Particle size/Sieved range (mm)	1.77/(+1.18-2.36)	0.196
	3.56/(+2.36-4.75)	0.272
	7.13/(+4.75-9.50)	0.341
	11.75/(+9.50-14.00)	0.395
Density (kg/m3)	1,500	2,700
Moisture (wt%)	8-10%	-
Weight Percent (wt%)	2, 5, 10, 15%	-

The biomass is larger but lighter than the inert sand used, the particle size and density ratio for palm shell/sand are of about 5 -53 and 0.55 respectively.

C. Procedure

The procedures in determining the U_{mf} and U_{cf}, i.e. via fast and slow defluidization as in [5] are adopted for sand-palm shell mixtures. Both methods are based on the bed pressure drop profiles and differing only in terms of rate of defluidization.

On U_{mf} determination using fast defluidization method, the mixture is initially fluidized vigorously ($>U_{mf}$) to maximize particles mixing and to ensure constant bed pressure drop is established, in order to form the constant fluidized bed line. Thereafter, the bed is defluidized rapidly, at bed pressure drop values below fluidized state ($<U_{mf}$), such that the mixtures uniformity remains unchanged (since particles rearrangements are avoided). This is used to form the fixed bed line. The U_{mf} is then determined from the intersection point between the

[1] Experiments using static bed height of 0.3 – 0.5m performed in both compartments confirmed the same results.

fixed bed and constant fluidized bed lines. Meanwhile, in slow defluidization, a method used to determine U_{cf}, the approach is to allow gradual changes from fluidized bed condition to fixed bed state. U_{cf} is determined from the point when the bed pressure drop is constant.

III. Results And Discussions

Fig. 4 shows the typical sand-palm shell bed pressure drop profile for U_{mf} and U_{cf}, obtained from palm shell of 4.75-9.50mm at 5 wt% in fine sand of 196µm in the combustor. This sand-palm shell mixture demonstrates similar profile as obtained in the previous pure sand bed [5] thus, permitting the identification of characteristic velocities using the same methods.

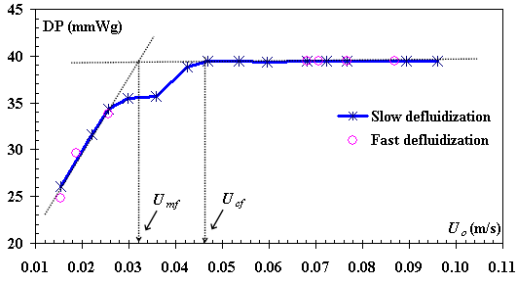

Figure 4: Typical sand-palm shell bed pressure drop profile for U_{mf} and U_{cf}

However, unlike single component system, depending on the palm shell size and composition in sand, the mixtures may exhibit severe segregating condition that leads to channeling. This condition is often observed for biomass-sand fluidization [10]-[11]. This behavior can be identified from distinctive pattern of the pressure drop profile. As shown in Fig. 5, during fast defluidization, the bed pressure drop at fluidized state shows a significantly lower steady state value (<70%) than those obtained from experiments where proper fluidization are attained. Furthermore, during slow defluidization, the steady state bed pressure drop cannot be established at fluidized state. In fact, the bed pressure drop profile is showing an upward trend. Both behaviors are analogous to that observed in a single component system that exhibits partial fluidization. Besides, visual observation also confirmed the presence of stationary portion of palm shell "chunks" in the vigorously fluidized bed. The profile shown below is obtained from palm shell of 4.75-9.50mm at 15 wt% in fine sand of 196µm in the combustor.

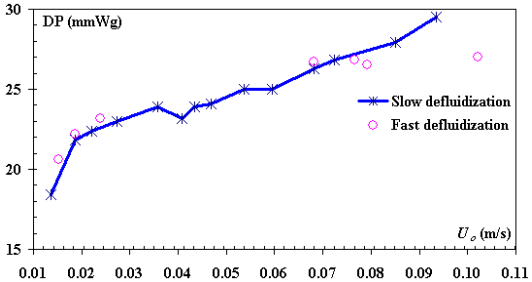

Figure 5. Typical sand-palm shell channeling bed pressure drop profile

It is worthy to be mentioned here that the maximum air flow (compressor capacity) has been supplied in all experiments where the bed pressure drop profiles are similar to Fig. 5. In this particular experiment, the maximum superficial velocity was at 0.221m/s, corresponding to about 10 times of the pure sand U_{mf}, producing a turbulent bed. Even at this condition, the mixtures fluidization was unsatisfactory with palm shell forming an immobile section inside a fluidized bed.

These two behaviors and bed pressure drop profiles are similarly observed throughout the experimental range in both of the compartments. Consequently, only those bed pressure profiles that show steady state values at fluidized condition for both defluidization methods are reported for their U_{mf} and U_{cf} values. It is important to note that through the implementation of both defluidization methods, segregation of palm-shell in the mixtures can be identified. This provides practical information on the maximum tolerable quantity of palm shell that can be fed during startup or that can be presence in the fluidized bed during operation.

A. *Effect Mixture Properties*

Fig. 6(a) and 6(b) show the effective density and particle diameter for mixtures of various palm shell size and weight percent in sand computed using the following weighted average mixtures properties:

$$\frac{1}{\rho_m} = \frac{\overline{w_s}}{\rho_s} + \frac{\overline{w_p}}{\rho_p} \quad (1)$$

$$\frac{1}{d_m} = \rho_m \left[\frac{\overline{w_s}}{\rho_s d_s} + \frac{\overline{w_p}}{\rho_p d_p} \right] \quad (2)$$

Fig. 6(a) shows slightly greater incremental magnitude in effective particle diameter as compared to the reduction of the effective density in Fig. 6(b). Consequently, when referring to the Ergun equation for U_{mf} prediction, there is a general expectation of incremental trends in U_{mf} (and U_{cf}) of sand-palm shell mixtures with the addition/increasing palm shell composition in the mixtures [12].

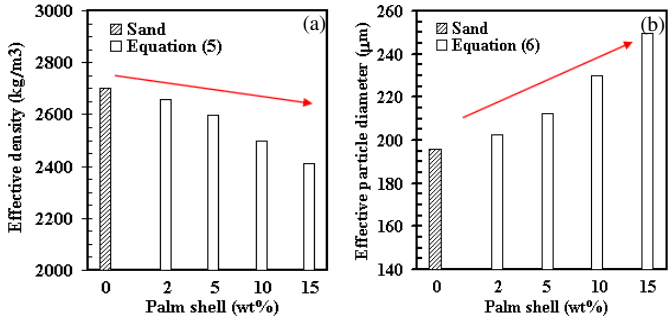

Figure 6: Effective mixture properties of various palm shell weight percent; palm shell of +1.18-2.36µm, sand of 196µm

The subsequent paragraphs describe the experiment results for these specific studies with respect to the effect of palm shell weight percent and sizes as well as the sand sizes in the mixture.

B. *Effect of Palm Shell Weight Percent*

As shown in Table II, increase of palm shell weight percent increases both the U_{mf} and U_{cf} values, in both of the compartment, following the increase of effective particle diameter of the mixtures.

TABLE II. CHARACTERISTIC VELOCITIES OF SAND–PALM SHELL (341μm; +9.50-14.00mm).

Compartment	**Combustor; (Gasifier)**			
Effective particle diameter (μm)	353	372	407	445
Palm shell (wt%)	2	5	10	15
U_{mf} (m/s)	0.084; (0.116)	0.095; (0.122)	0.100; (0.138)	0.106; (0.166)
U_{cf} (m/s)	0.087; (0.167)	0.102; (0.166)	0.111; (0.180)	0.127; (0.258)

C. *Effect of Palm Shell Size*

Table III shows that both the U_{mf} and U_{cf} increases with the increase of palm shell size in both compartments and also in tandem with the increase of effective particle diameter.

TABLE III. CHARACTERISTIC VELOCITIES OF SAND-PALM SHELL (272μm;10wt%)

Palm shell size (mm)	Effective particle diameter (μm)	Combustor Characteristic Velocity (m/s)		Gasifier Characteristic Velocity (m/s)	
		U_{mf}	U_{cf}	U_{mf}	U_{cf}
+1.18-2.36	317	0.054	0.066	0.084	0.090
+2.36-4.75	321	0.054	0.068	0.082	0.091
+4.75-9.50	324	0.065	0.090	0.079	0.129
+9.50-14.00	325	0.074	0.114	0.180	0.188

D. *Effect of Sand Size*

Increasing the sand size in the sand-palm shell mixtures increases the mean particle diameter as shown in the Fig. 7 computed based on (2). Consequently, one would expect the incremental trend of the mixtures characteristic velocities. This is true when fluidization is dominated by gas-particle interaction.

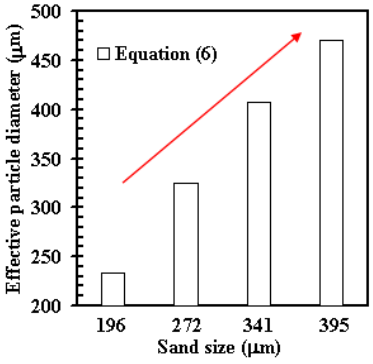

Figure 7: Effective particle diameter for various sand sizes;

palm shell of +9.50-14.00mm, 10wt%

Although some of the data such as those presented in Table IV demonstrate this general tendency of incremental U_{mf} and U_{cf}, the opposite trends of decreasing U_{mf} and U_{cf} values are also observed as shown in Table V.

TABLE IV. U_{mf} AND U_{cf} FOR PALM SHELL +4.75-9.50mm AT 5wt%

Sand size (μm)	**Combustor Characteristic Velocity (m/s)**		**Gasifier Characteristic Velocity (m/s)**	
	U_{mf}	U_{cf}	U_{mf}	U_{cf}
196	0.032	0.043	-	-
272	0.057	0.072	0.081	0.098
341	0.072	0.087	0.115	0.132
395	0.083	0.097	0.107	0.136

TABLE V. U_{mf} AND U_{cf} FOR PALM SHELL +9.50-14.00mm AT 5wt%

Sand size (μm)	**Combustor Characteristic Velocity (m/s)**		**Gasifier Characteristic Velocity (m/s)**	
	U_{mf}	U_{cf}	U_{mf}	U_{cf}
196	-	-	-	-
272	0.082	0.114	0.180	0.191
341	0.099	0.111	0.138	0.180
395	0.082	0.097	0.124	0.167

E. *Analysis on Charateristic Velocities*

1) *Ratio of Characteristic Velocity (Mixture/Sand)*

When representing these data in dimensionless ratio, i.e. U_{mf}/U_{mf}^{o} and U_{cf}/U_{cf}^{o} where the denominators are the characteristic velocities of pure sand [5], a distinct pattern revealed. As Table VI and VII shown, these ratios in fact are in trends of reducing with the increase of sand size in the mixture. These patterns are observed in all experiments with more noticeable trend at largest palm shell size of +9.50-14.00mm.

TABLE VI. DIMENSIONLESS VELOCITES FOR SAND-PALM SHELL (+4.75-9.50mm, 5wt%)

Sand size (μm)	**Combustor Dimensionless Velocity (m/s)**		**Gasifier Dimensionless Velocity (m/s)**	
	U_{mf}/U_{mf}^{o}	U_{cf}/U_{cf}^{o}	U_{mf}/U_{mf}^{o}	U_{cf}/U_{cf}^{o}
196	1.52	1.43	-	-
272	1.08	1.12	1.05	1.13
341	0.99	1.02	1.13	1.13
395	1.00	0.93	1.02	1.12

TABLE VII. DIMENSIONLESS VELOCITIES FOR SAND-PALM SHELL (+9.50-14.00mm , 10wt%)

Sand size (μm)	**Combustor Dimensionless Velocity (m/s)**		**Gasifier Dimensionless Velocity (m/s)**	
	U_{mf}/U_{mf}^{o}	U_{cf}/U_{cf}^{o}	U_{mf}/U_{mf}^{o}	U_{cf}/U_{cf}^{o}
196	-	-	-	-
272	1.55	1.78	2.34	2.20
341	1.36	1.31	1.35	1.54
395	0.99	0.93	1.16	1.38

Fig. 8 and 9 show the dimensionless velocities ratio in the combustor for different palm shell size and weight percent.

The trends of reducing ratio with increase of sand size also prevail for palm shell of 5 – 15 wt% in both palm shell sizes.

Data for mixtures consist of palm shell at 2 wt% are not included in Fig. 8–11 to allow better visualization of the trends, since they generally do not vary appreciably from pure sand. This is expected as the proportion of palm shell is too small when compared to the sand amount in the bed. These data are reported later (Part II of this paper).

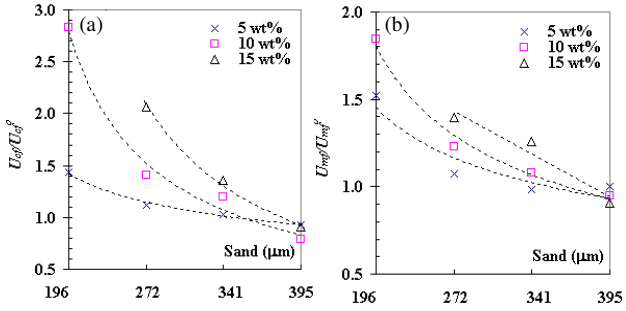

Figure 8(a) and 8(b): Dimensionless velocities in the combustor; palm shell of +4.75-9.50mm at 5-15 wt%

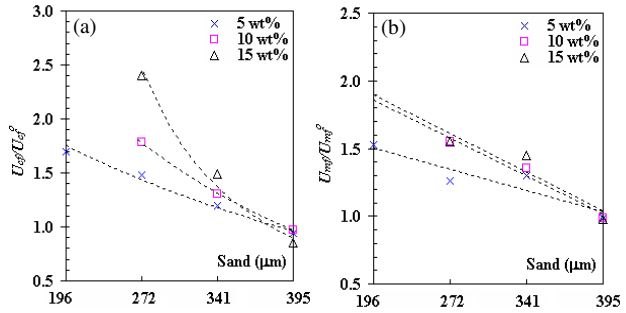

Figure 9(a) and 9(b): Dimensionless velocities in the combustor; palm shell of +9.50-14.00mm at 5-15 wt%

In addition, it has been shown earlier that in the effect of palm shell proportion, higher palm shell weight percent leads to higher characteristic velocities for given sand in the mixtures. Consequently, the ratio of U_{mf}/U_{mf}^{o} and U_{cf}/U_{cf}^{o} also increases with the present of more palm shell in the mixture, such as the data shown in Fig. 8 and 9 for sand of 272 µm.

However, this ratio gradually reduce when larger sand is used and approaches unity for the largest sand, i.e. at 395µm, this simply means that the mixtures U_{mf} and U_{cf} are essentially of the pure sand used.

Fig. 10 and 11 display the results of the dimensionless velocities in the gasifier for the same sand-palm shell mixtures in the combustor. Although similar trends are also obtained in the gasifier as Fig. 10 and 11 shown, the degree of reducing differences particularly in the U_{cf}/U_{cf}^{o} (refer Figure 8(a) and 9(a)) when larger sand is used is not as profound as in the combustor. It can be seen that the U_{cf}/U_{cf}^{o} for palm shell of 15wt% in both Figures 10(a) and 11(a) do not depreciate but are very close for all the sand sizes. Moreover, both the dimensionless velocities ratios do not converge to unity for the largest sand used in the mixtures.

The analysis carried out for the fluidization of pure sand has confirmed that the characteristic velocities of the gasifier (distinctive from the combustor) are affected by the compartment diameter and larger particle-to-bed-diameter ratio, these being related to wall effect [5].

Indeed, the present studies further support the findings from L.R. Glicksman and G. Mc. Andrews [13] and J. Werther [14] whom shown that the hydrodynamic of gas-solid fluidized bed (bubble characteristic) are influenced by the wall spacing when the spacing is less than 40-50cm.

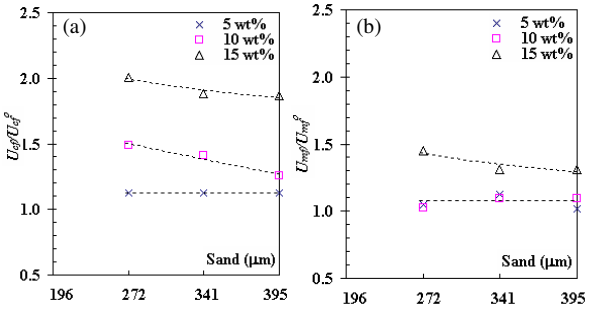

Figure 10(a) and 11(b): Dimensionless velocities in the gasifier; palm shell of +4.75-9.50mm at 5-15 wt%

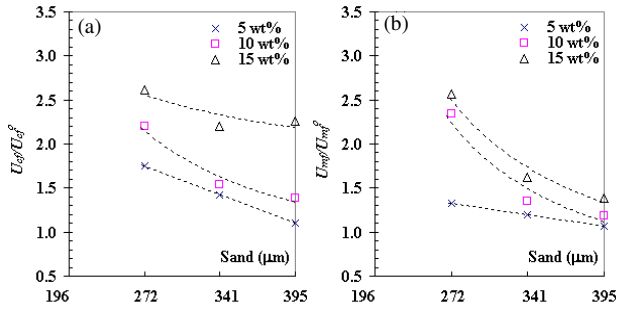

Figure 10(a) and 11(b): Dimensionless velocities in the gasifier; palm shell of +9.50-14.00mm at 5-15 wt%.

To distinguish the fluidization behavior obtained in the combustor and gasifier, a brief description on the mechanism of particle fluidization is included here.

2) Particle Fluidization Mechanism

The mechanism of attaining particle fluidization depends on both the contributions of gas-particle and particle-particle interaction.

R. Clift et al. [15] described the gas-particle interaction is the buoyancy force acted on the particle in a fluidized suspension or the net effect of fluid drag and gravitational forces. As mentioned, palm shell on its own could not be fluidized. According to Chiba and Nienow [16], the gas-particle interaction in the binary mixture occurs with the transport of jetsam particles in the bubble wakes of the fluidized bed.

On the other hand, the particle-particle interaction is the collision of jetsam-to-flotsam i.e. sand-palm shell particle for the case of binary mixture. Collision of the same type (jetsam-to-jetsam or flotsam-to-flotsam) has net zero collision interaction. However, the interaction forces between particles

are very complicated and subjected to the mixing/segregation condition in the mixtures. Most authors agreed the particle mixing is enhanced with the reduction of particle size ratio (jetsam/flotsam) and/or the increase of bubble diameter (that is a proportional to the column diameter).

3) Excess Gas Velocity

The difference between mixture U_{cf} and U_{mf} provides an indication of the excess gas velocity available. This excess gas velocity if available may contribute to the increase of gas-particle interaction i.e. drag force > gravitational force for sand in the mixture.

Fig. 12 shows the differences between the mixture U_{cf} and U_{mf} for palm shell of +4.75-9.50mm and +9.50-14.00mm respectively in the combustor. These trends clearly show that the differences in characteristic velocity reduce with the increase of sand size, except at palm shell of 5 wt%, the values remain nearly constant. Similar results are obtained for palm shell of +9.50-14.00mm. Consequently, the observations reported in Table VI and VII are very unlikely due to the excess gas availability, instead attributed to the increase in the particle-particle collision of sand-palm shell mixtures in achieving fluidization.

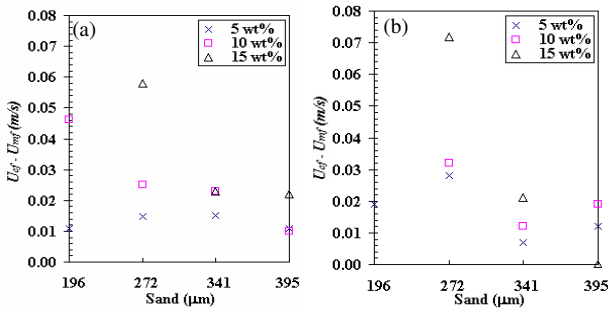

Figure 12: Difference of characteristic velocity in the combustor; palm shell of (a) +4.75-9.50mm and (b) +9.50-14.00mm at various weight percent

Fig. 13(a) and 13(b) show the differences between the mixture U_{cf} and U_{mf} for palm shell of +4.75-9.50mm and +9.50-14.00mm respectively in the gasifier. On the contrary, the results for the gasifier show generally an upward trend with the increase of sand size. Higher gas-particle interaction is necessary to establish mixture fluidization apart from the contribution of particle-particle interaction in the gasifier. The former is needed to supplement the latter in achieving stable fluidization, despite of the increase in particle-particle interaction with the increase of sand size. This can be explained by the propensity of mixing/segregation in the gasifier.

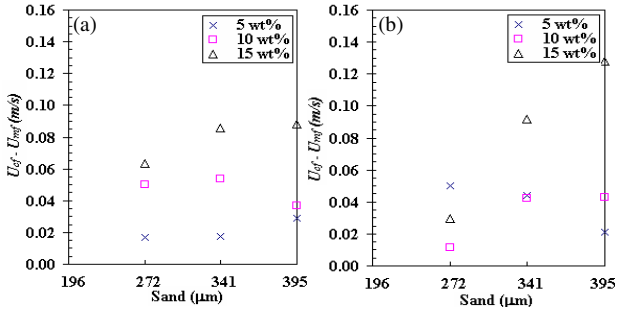

Figure 13(a) and 13(b): Difference of characteristic velocity in the gasifier; palm shell of +4.75-9.50mm and +9.50-14.00mm at various weight percent

According to the bubble growth criterion, for the same superficial velocity, the smaller diameter column produces smaller bubble diameter compared to the larger column. Hence, it can be expected that the mixing tendency, induced by the bubble activities is less effective in the gasifier as compared to the combustor. Consequently, the formation of segregated portion in the gasifier is enhanced, thus reduces the relative motion of the trapped particles and finally diminishes the supposedly much larger contribution of particle-particle interaction.

In addition, palm shell size of 20-30 times larger than sand have the tendency to "hook up" together, forming even bigger chunk of particles that must be broken in order to attain or sustain fluidization. This behavior of particles interlocking with each other to form larger particles during fluidization has been cited in the work from R.R. Pattipati and C.Y. Wen [17]. The greater the proportion of palm shell in the mixture would indefinitely leads to greater likelihood of such formation or larger chunk formation. As a result, to establish fluidization, a greater superficial velocity is essential not only to overcome the gravitational force but also to break through the suppression of the surrounding palm shell chunks.

This is supported by the observation of U_{cf}/U_{cf}^{o} values for palm shell of 15wt% in both Fig. 10(a) and 11(a) that do not depreciate but are very close for all the sand sizes. Moreover, such as the case of fine sand (196μm) and palm shell mixtures in the gasifier, the smaller particle size ratio has resulted in the smaller contribution of particle-particle interaction. Segregation is also more severe due to the smaller column diameter (with smaller bubble diameter). The trapped particles in the segregated portion reduce further the contribution of particle-particle interaction for fluidization. As a result, channeling prevails even when the mixtures is subjected to the maximum available air flow ($10U_{mf}$ of fine sand (196μm)) in the present setup.

4) Ratio of Mixture Characteristic Velocity

Meanwhile, for a given system, $U_{cf}/U_{mf} = 1$ is established when the bed material is perfectly mixed during defluidization. Hence, this ratio is also an indication of the extent of segregation.

Contrary to the U_{cf}/U_{mf} ratio for pure sand component that is approximately constant with increasing sand size [5], Fig. 14(a) and 14(b) show that for the sand/palm shell mixtures, these ratios reduce and approach to unity with the increase of

sand size in the mixtures in the combustor, except for palm shell of +4.75-9.50mm at 5wt%, where its result is very close to the pure sand value. Similar trends are cited in [11] using biomass-sand mixtures.

These shows that the bed homogeneity has gradually improved with the reduction of particle size ratio, despite having to be 20-30 times greater than the typical large-to-fine particle size ratio (<√2) recommended by Wen and Yu [18] for good mixing.

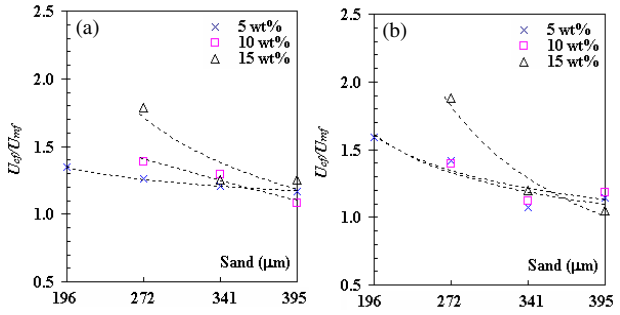

Figure 14(a) and 14(b): Dimensionless velocities in combustor; palm shell sizes (a) +4.75-9.50mm and (b) is +9.50-14.00mm at various weight percent

It is known that for any multi-components system differing in both particle densities and sizes, the larger and denser components tend to sink while the smaller and lighter components tend to float forming two segregated parts. In this case, mixing effect is suppressed and the system may exhibit either as density-segregating or size-segregating mixtures [19]. However, in the present system, palm shell is larger *but* lighter than sand in the mixtures. Consequently, the tendencies of palm shell to sink or float in the mixture vary depending on its particle size and density. In addition, the action of segregating factors may tend to either strengthen or counterbalance that of the other.

The extremely large particle size ratio of palm shell and sand (up to 53) suggests that the size-segregating factor is dominate and hence palm shell tends to be the jetsam instead (such in the case of largest palm shell and finest sand). This has caused severe channeling and the mixture exhibits a bed pressure profile similar to Figure 5.0. However, with the increase of sand size (or reduction of palm shell size), this size ratio reduces and the tendency for palm shell to float is gradually enhanced. It is known that incipient bed voidage of a fluidized bed composing of sand generally decreases with the increase of sand size [20]. While sand is already the heavier component in this mixture, the increase in sand size may lead to the increase in local bulk density (a function of incipient bed voidage). When the bulk density is higher than the palm shell particle density, palm shell tends to be the flotsam. Hence, at the point where these contributions are sufficiently large to counterbalance size-segregating factor, palm shell/sand mixture is capable of forming a homogenous bed at U_{mf} and U_{cf}. B. Carter et al. [21] have described this behaviour as loosely analogous to "buoyancy" in their experiments of large particle coal sintered ash of 5 – 15mm in sand.

Meanwhile, this condition depends not only to the particle size ratio, but also to the palm shell composition in the sand. As shown in Figure 14(a) and 14(b), the U_{cf}/U_{mf} generally increases with the palm shell weight percent in a given sand size. In Figure 14(a), for palm shell of 5wt%, the U_{cf}/U_{mf} values remain nearly constant at various sand sizes. The effect observed is in total agreement with Formisani et al. [19] results where for fully dissimilar solids, the U_{cf}/U_{mf} values are identical at low fraction of the jetsam component in the binary mixtures.

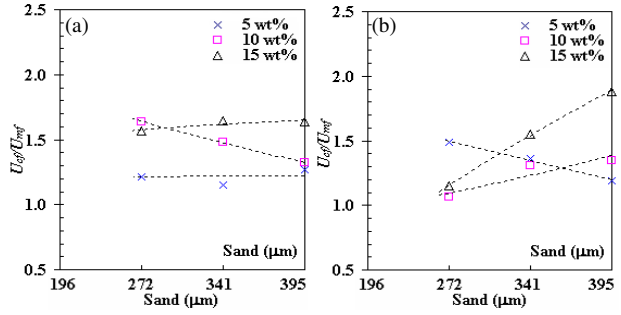

Figure 15(a) and 15(b): Dimensionless velocities in the gasifier; palm shell sizes (a) +4.75-9.50mm and (b) +9.50-14.00mm at various weight percent.

However, the U_{cf}/U_{mf} trends observed in the gasifier are more complex from those found in the combustor due to the present of significant bed geometrical effect, where its intensity varies with the particle size and composition. As Fig. 15(a) shown, for smaller palm shell of +4.75-9.00mm at 5 wt%, the U_{cf}/U_{mf} is approximately constant with results very closely to the pure sand condition in [5]. At palm shell of 10 wt%, the U_{cf}/U_{mf} ratio reduces with the increase of sand size; a tendency resembles to those found in the combustor and thus depends on the same effects described earlier. Similar trend is observed in Fig. 15(b) when larger palm shell of +9.50-14.00mm is at 5 wt%.

To the contrary, at palm shell of 15wt%, Fig. 15(a) shows an incremental U_{cf}/U_{mf} ratio with the increase of sand size. The same trends are observed at 10 and 15 wt% for palm shell of +9.50-14.00mm as shown in Fig. 15(b). These increasing ratios show that segregation of bed mixture is enhanced with the increase of palm shell in size and weight percent.

IV. CONCLUSION

In short, it has been shown that the methodology developed in the cylindrical column for the determination of the fluidization behaviour and characteristic velocities can be implemented in the present compartmentalized reactor design and with sand/palm shell binary mixtures.

On one hand, using smaller sand particle reduces the superficial velocity necessary to establish fluidization when the palm shell components are smaller in sizes or weight percent in the mixtures. However, the tendency for segregation to occur is higher when the resulting particle size ratio (palm shell/sand) is higher due to the lower contribution of particle-particle collision. Consequently, higher superficial velocities are necessary to fluidize the bed mixtures especially if there is any formation of palm shell "chunks" that is enhanced by the present of larger palm shell size and weight

percent. Particle segregation is further promoted when the column diameter is small.

To the contrary, when utilizing large sand particle in the mixture, although greater superficial velocity is required as compared to smaller sand size in order to establish fluidization when palm shell is smaller in sizes or weight percent, the tendency for segregation to occur reduces when the resulting particle size ratio is lower due to the greater contribution of particle-particle collision.

Overall, the studies on the U_{mf} and U_{cf} values as well as the bed pressure drop profiles of sand-palm shell mixtures have certainly provide insight on the fluidization behaviour and the mixing/segregation tendency. These findings prove that the characteristic velocities of the sand-palm shell binary mixtures not only depend on the effective bed properties, but also influenced by the mixing/segregating condition. In addition, the bed geometry is an equally important factor for the present system.

ACKNOWLEDGMENT

Authors would like to thank the research students who assist in performing the experimental works.

REFERENCES

[1] T.L.Kelly-Yong, K.T. Lee, A.R. Mohamed and S. Bhatia, "Potential of hydrogen from oil palm biomass as a source of renewable energy worldwide," Energy Policy, 2007, vol.35, pp. 5692–5701.

[2] S.H. Shuit, K.T. Tan, K.T. Lee and A.H. Kamaruddin, "Oil palm biomass as a sustainable energy source: A Malaysian case study," Energy, 2009, vol. 34, pp. 1225–1235.

[3] H.P Yang, R. Yan, H.P Chen, D.H.Lee, D. T. Liang and C.G. Zheng, "Pyrolysis of palm oil wastes for enhanced production of hydrogen rich gases," Fuel Processing Technology, 2006, vol. 87, pp. 935–942.

[4] J. Guo and and A.C. Lua, "Preparation and characterization of adsorbents from oil plam fruit solid waste,", Journal of Oil Palm Research, 2000, Vol. 12 (1), pp- 64-70.

[5] V.S. Chok, S.K. Wee, A. Gorin and H.B. Chua, "Effect of particle and bed diameter on characteristic velocities in Compartmented Fluidized Bed Gasifier," 2nd CUTSE International Conference: Progress in Science and Engineering for Sustainable Development, 24-25th November 2009, unpublished.

[6] P.N. Rowe and A.W. Nienow, "Particle mixing and segregation in gas fluidised beds. A review," Powder Technology, 1976, vol. 15, pp. 141-147.

[7] V.S. Chok, L.F.B. Chin, S.K. Wee, W.W. Tang, A. Gorin, H.B. Chua and H.M. Yan, "Hydrodynamics studies of sand/palm shells binary mixtures in compartmented fluidized bed gasifier (CFBG)," 1st Engineering Conference on Energy & Environment (EnCon), UNIMAS, Kuching, Sarawak, December 2007.

[8] M. Fauziah, A.R. Nornizar, A. Nornizar, A. Azil Bahari and M.J. Tajuddin,"Cold flow binary fluidization of oil palm residues mixture in a gas-solid fluidized bed system," Pertanika Journal of Science and Technologi, 2008, vol. 16(2), pp. 201-212.

[9] S.K. Wee, V.S. Chok, L.F.B. Chin, W.W. Tang, A. Gorin, H.B. Chua and H.M. Yan, "On the effect of effective diameter on fluidization quality in compartmented fluidized bed gasifier," Pertanika Journal of Science & Technology, vol. 17(2), 2009, pp. 347-354.

[10] R. Bilbao, J. Lezaun and J.C. Abanades, "Fluidization velocities of sand/straw binary mixtures," Powder Technology, 1987, vol. 52, pp. 1-6.

[11] M. Pilar Aznar, F.A. Gracia-Gorria and J. Corella, "Minimum and maximum velocities for fluidization for mixtures of agricultural and forest residues with a second fluidized solid. I. Preliminary data and results with sand-sawdust mixtures," International Chemical Engineering, 1992, vol. 32 (1), pp. 95-102.

[12] Fluidization Engineering, 2nd Edition, Kunii and Levenspiel, Butterworth-Heinemann, pp. 71-72, 1991

[13] L.R. Glicksman and G. Mc. Andrews, "The effect of bed width on the hydrodynamics of large particle fluidized beds," Powder Technology, 1985, vol. 42, pp. 159-167.

[14] J. Werther, "Influence of the Bed Diameter on the Hydrodynamics of Gas Fluidized Beds," 1968, *AIChE Symposium Series*, Vol. 70(141), pp. 53-62.

[15] R. Clift, J.P.K Seville, S.C. Moore and C. Chavarie, "Comments on the buoyancy force on the particles in a fluidized suspension," Chemical Engineering Science, 1987, vol. 42(1), pp. 191-194.

[16] T. Chiba and A.W. Nienow, in D. Kunii and R. Toei (eds.), Fluidization IV, Engineering Foundation, New York, 1984, p. 195.

[17] R.R. Pattipati and C.Y. Wen, Minimum fluidization velocity at high temperatures, Industrial Engineering and Chemical Process Design and Development, 1981, vol. 20, pp. 705-708.

[18] C.Y. Wen and Y. H., "A generalized method for predicting the minimum fluidization velocity," AICHE Journal, vol. 12(3), pp. 610-612.

[19] B. Formisani, R. Girimonte and T. Longo, "The fluidization process of binary mixtures of solids: Development of the approach based on the fluidization velocity interval," Powder Technology, 2008, vol. 185 (2), pp. 97-108.

[20] D. Kunni and O. Levenspiel, Fluidization Engineering, 2nd Edition, Butterworth-Heinemann, 1991, pp. 69

[21] B. Carter, M. Ghadiri and R. Clift, "The behavior of large jetsam particles in fluidised beds," Powder Technology, 1987, vol. 52, pp. 263-266.